JOURNAL OF MATERIALS SCIENCE 28 (1993) 3035–3042

Fracture process of superdrawn polyoxymethylene fibres

T. KOMATSU
Analytical Research Centre of Asahi Chemical Industry Co. Ltd, 2-1 Samejima, Fuji, Sizuoka 416, Japan

A fracture process of superdrawn polyoxymethylene fibres was studied in terms of the structural deformation under stress by scanning electron microscopy. The fibrillar structure consisted of two structural units showing different stress–fracture behaviour, i.e. one was a linear void-chain connected to thin cross-fibrils which was fragile to tensile stress; the other was a network of thick fibrils which was very resistant to stress and prevent lateral development of void-fracture. Fracture began from a dominant fracture of void-chains followed by a fibrillar fracture at the micronecks, i.e. a shear band fracture. This process was clearly due to the above fibrillar structure including voids. Void-fracture hardly influenced fibrillar fracture, suggesting a possible dependence of the dimensions of the frame fibrils on fracture strength. Also, the fracture process clearly included fibrillar slippage and heat generation.

1. Introduction

Fibrillar structure and the fracture process of highly oriented polymer fibres have been studied to explain the enhancement and limits in mechanical properties, including tensile strength, from various viewpoints, such as fracture mechanics, statistical/stochastic theory, kinetic rate theory and thermodynamics. A fracture theory of materials appeared in Griffith's work on the fracture of glass fibres [1], which established linear elastic fracture mechanics for metallic materials [2, 3], and was applied to fatigue and creep fractures of polymer materials [4]. Polymer fibres are ductile or tougher materials different from inorganic material. Fracture toughening of fibres has been recently interpreted as crack shielding effects [5].

An original stochastic approach to polymer fractures has been introduced in Pierce's weakest link hypothesis as the stochastic technique to determine defects having a maximum size, i.e. a minimum strength, in the distribution of defects linearly linked [6]. A statistical/stochastic theory was developed using the Weibull model of flaw population [7]. A size effect in tensile strength derived from the theory has been discussed for Kevlar and ultrahigh molecular weight polyethylene (UHMWPE) fibres [8].

The mechanism of cavitation leading to ultimate fracture of polymer fibres has been discussed in terms of the kinetic rate theory and the absolute reaction rate theory [9–11]. The approach is based on the experimental results of free radical generation during fracture, assuming the primary or secondary bond scission of tie molecules to cause the formation of submicrocracks. The mechanism thus requires the dependence of free radicals and microdefects on strain and this has been experimentally confirmed [12–14]. In addition, the theoretical dependence of time to failure on stress, has been applied to creep fracture of polymer fibres and explains the experimental results well [15–17]. These studies led to an approach for obtaining the ultimate tensile strength of perfect fibres, which combines the kinetic rate theory and simulation of the stress–strain relation using a stochastic Monte Carlo process [18]. These approaches are mainly based on two assumptions: (1) ultimate fracture occurs just when all chains in the cross-section are ruptured; (2) the chain scission results from breakage of primary and secondary bonds (in the assumptions, the value of activation energy for the primary bond is also important, but too small compared to the dissociation energy of the C–C covalent bond).

Real fracture is governed by defects generated locally on the fibre surface. Stress concentration around the defects thus does not lead to complete breakage of all molecular chain bonds throughout the sample, i.e. the fracture process is heterogeneous and includes the possibility of slippage of fibrils or molecular chains in addition to bond dissociation. Therefore, these approaches are not very useful to explain real fibre fracture.

The nucleation theory premising a heterogeneous nucleation process [19, 20], may improve the kinetic theory, including the above unrealistic assumptions. The activation energy for creep fracture of UHMWPE fibres obtained according to the nucleation theory, was about one-quarter of the C–C covalent bond. It was then clarified that strength was mainly determined by intermolecular bonds [21]. The dependence of tensile strength of UHMWPE fibres on fibrillar aspect ratios has also been discussed using a matrix model of reinforced materials with the fibrillar structure. It was then suggested that strength depended on the number of interfibrillar bonds [22].

0022–2461

A thermodynamic approach to fracture is given in the theory of phase equilibrium in necking [23], leading to the idea of a crystal–melt phase transition by a tensile load [24]. This idea does not require free radical generation of fracture and suggests that the fracture of real fibres may be interpreted in terms of interfibrillar bond energy. Fracture has also been studied by an electron microscopic approach to observe structural deformation under compression in real time [25]. Fractography for analysis of the fracture process of plastics [26, 27] is also effective for superdrawn fibres [21, 28–30]. For example, the fracture of the UHMWPE fibres has been shown to be initiated at surface irregularities such as kink bands [21].

A certain theory or hypothesis may be useful for discussing the fracture process and ultimate strength of the perfect polyethylene fibre, but no theories have been proposed to explain well the fracture process and ultimate strength of fibres having finite molecular weight and imperfect structure, orientation and crystallinity, because fractures of these fibres are governed mostly by various kinds of structural heterogeneities or defects such as voids, kink bands, trapped entanglements, chain ends, misalignment, and the deformation of such defects in tension, rather than covalent bonds in the chain. The difficulty of analysis of the fracture process of real oriented fibres seems mainly to arise from (1) a defective fibrillar structure characterized by processing [30] and polymer species [31–34], (2) fracture which does not proceed according to a fixed mode but by complex combinations of various processes. Accordingly, analysis of the change in fibrillar structure under stress is a basis for studying the fracture process of real fibres.

In this paper, the fracture process at the initial stage at the surface of superdrawn polyoxymethylene fibres is discussed with respect to the deformation of fibrillar structure under tension which was examined in detail by scanning electron microscopy (SEM).

2. Experimental procedure

2.1. Sample preparation

A highly drawn polyoxymethylene fibre was continuously prepared by pressurized two-stage drawing using an undrawn tube of outer diameter 1.5 mm and inner diameter 0.5 mm from acetal homopolymer "Tenac 3010" (Asahi Chemical Industry Co. Ltd) and followed by completely removing any silicone oil adhering to the fibre. The drawing conditions were as follows: in the first stage, the vessel length was 12 m, the feed speed was 0.5 m min^{-1}, the draw ratio was 8, the drawing temperature was 150 °C, and the gauge pressure was 50 kg cm^{-1}; in the second stage, the vessel length was 45 m, the drawing temperature was 170 °C, the gauge pressure was 200 kg cm^{-1} and the total draw ratio was 30. The details for this procedure were previously described [34].

A fractured sample was prepared by stretching the fibre to fracture at room temperature on an Instron tensile testing machine using two stainless reel chucks of 160 mm diameter. The sample length (the distance between the centres of the reels) was 200 mm and the crosshead speed was 1 mm min^{-1}. A stretched sample was prepared as follows: the fibre was stretched once at a crosshead speed of 1 mm min^{-1} to the level of 80%, 90% or 95% breaking stress, and then the stress was removed immediately by raising the crosshead at the same speed.

2.2. Sample preparation for SEM observation

The cross-section was prepared in the following way. The fibre was cut into pieces ~20 mm long, immersed in di-glycidyl ether and infiltrated with the liquid by degassing under vacuum. The fibre was then immersed in the mixed solution consisting of an epoxy resin (Oukenn Syouji Co., "EPOC 812") (34 ml), *n*-methyamine (30 ml) and diglycidyl ether (64 ml) for 24 h, put into a gelatine capsule, filled with a portion of the mixed solution of the epoxy resin (34 ml), *n*-methylamine (30 ml) and tri-dimethyl amino methyl phenol (0.96 ml) and perfectly cured at 40 °C for 72 h. The resultant encapsuled fibre was cut in the middle with a jigsaw, trimmed in the cross-section of the fibre using a razor, smoothed with a glass knife and finished with a diamond knife. Next, the cured epoxy resin in the fibre was extracted with chloroform for 48 h using a Soxhlet's extractor.

2.3. SEM observation

The samples were lightly gold coated and examined by scanning electron microscopy (Hitachi Seisakusyo Co., S-430 operated at 5 kV).

3. Results and discussion

3.1. Fibrillar structure

It is supposed that tensile fracture of superdrawn polyoxymethylene fibres will be initiated at the surface defects, as has been found for highly oriented UHMWPE fibres [21]. Hence, a fibrillar structure in the fibre surface was first investigated. Fig. 1 shows a scanning electron micrograph of the surface of the original sample with a draw ratio of 30, Young's modulus of 59.5 GPa, tensile strength of 1.9 GPa, ultimate elongation of 5.5% and void-volume fraction of 32%. This shows the uppermost surface to be smooth and with few voids, in spite of the high void content in the bulk, and also indicates that the structure consists of fibrils parallel to the fibre axis, cross-fibrils like a ladder around voids which connect the neighbouring fibrils, and voids as spaces between the cross-fibrils. Fig. 2 shows scanning electron micrographs of the cross-section near the surface of the same sample, which reveals a complex structure of fibrillar networks. The network structure is characterized by a frame network of thick fibrils (trunk fibril), a sub-network of fibrils branching (branch fibril) inside a cell unit which forms the frame, and thin cross-fibrils and voids in the sub-network, being somewhat similar to that of the shells of a muskmelon or the veins of a leaf (Fig. 2a). The mean thicknesses of trunk, branch and cross-fibrils were approximately 1, 0.3, and 0.05 μm,

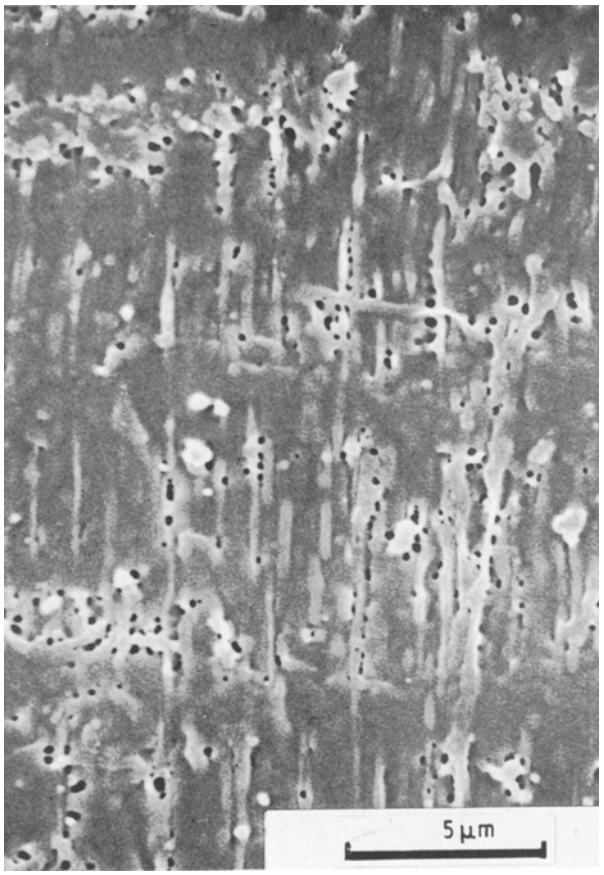

Figure 1 Scanning electron micrograph of the surface of a superdrawn POM fibre.

respectively, and the mean diameter of voids about 0.2 μm, as shown in Fig. 2b.

The combination of the surface and cross-sectional fibrillar structures also enables one to imagine a three-dimensional structure. Voids linking together in the longitudinal direction a linear void-chain, existing between fibrils, which is regarded as the smallest unit of the fibrillar structure or the minimum unit of defect structure. Each void in the chain is screened with thick fibrils and separated by thin cross-fibrils in directions parallel and perpendicular to the fibre axis, respectively. The void-chains link together along branch fibrils to form the sub-network, and the sub-networks cohere together in the frame network of trunk fibrils. It was also found that the fibre showed a so-called skin/core structure, i.e. very dense up to the depth of ~2 μm from the uppermost surface, but porous at a more interior point. It is due to this dense skin structure that few voids are observed in the intact sample surface.

3.2. Plastic deformation of the fibrillar structure

The deformation behaviour of voids up to tensile fracture provides some information on the fracture process. To investigate void deformation under stress, the applicability of the method to trace a compressive or stretching process of high-performance polymer fibres at real time [25] was examined. However, the present

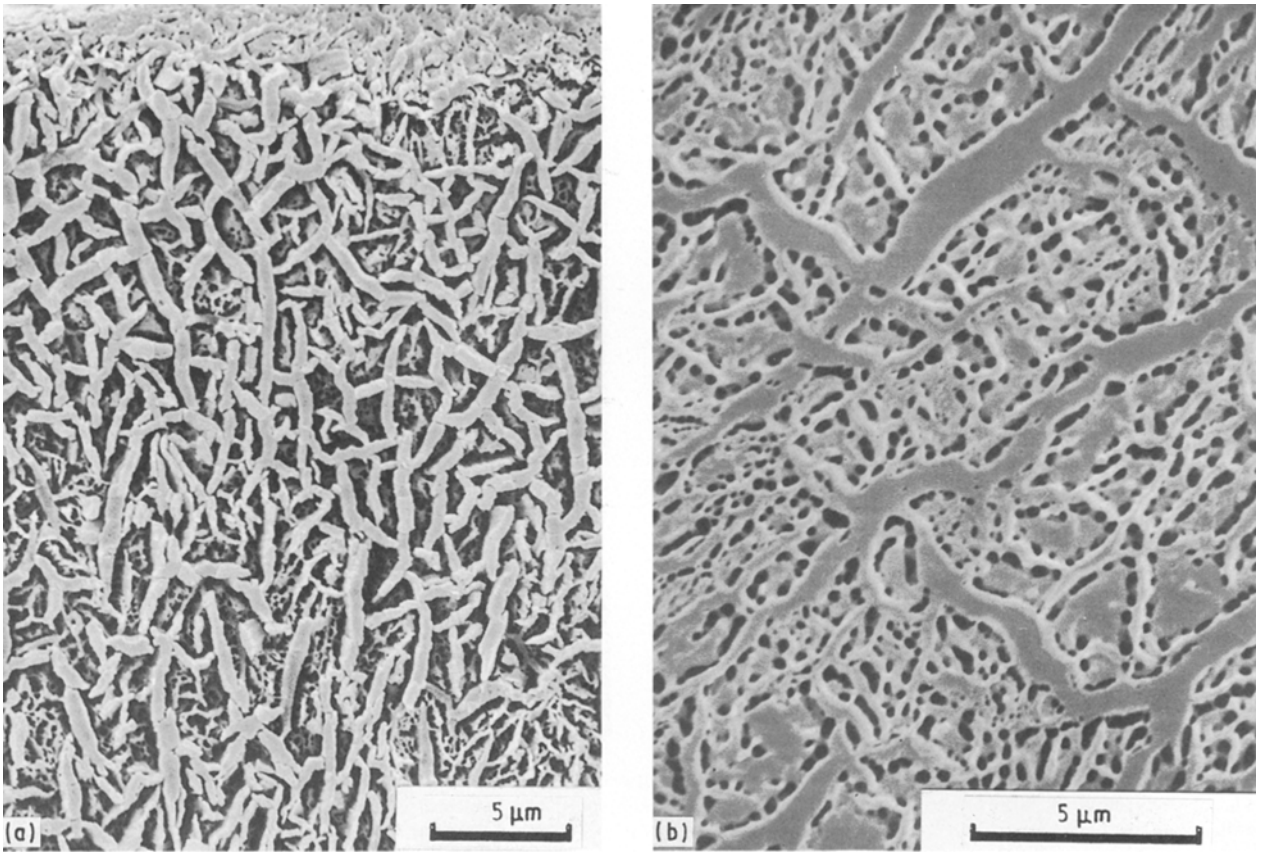

Figure 2 Scanning electron micrographs of the cross-section of a superdrawn POM fibre: (a) cross-section near the fibre surface; (b) cross-section at higher magnification.

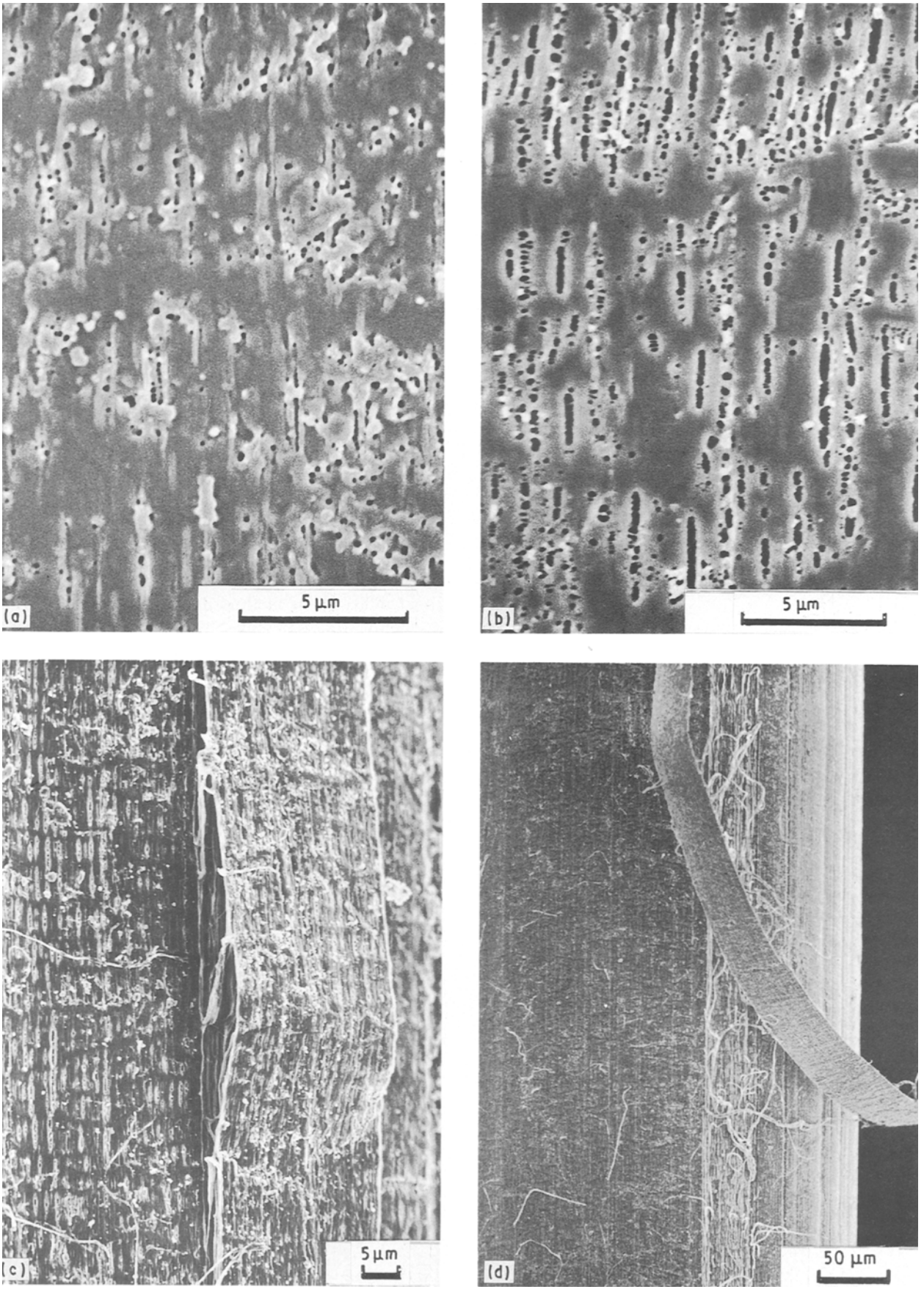

Figure 3 Scanning electron micrographs of the surfaces of stretched superdrawn POM fibres: (a) a stretched sample at 80% breaking strength; (b) a stretched sample at 90% breaking strength showing many slender voids; (c) a stretched sample at 90% breaking strength showing a fibrillar band just before fracture and an inclined shear band at the root; (d) a stretched sample at 95% breaking strength showing a fractured fibrillar band and its striated trace; (e) the opposite fracture surface of the fractured fibrillar band in (d); (f) a striated trace of the fractured fibrillar band in (d) at higher magnification.

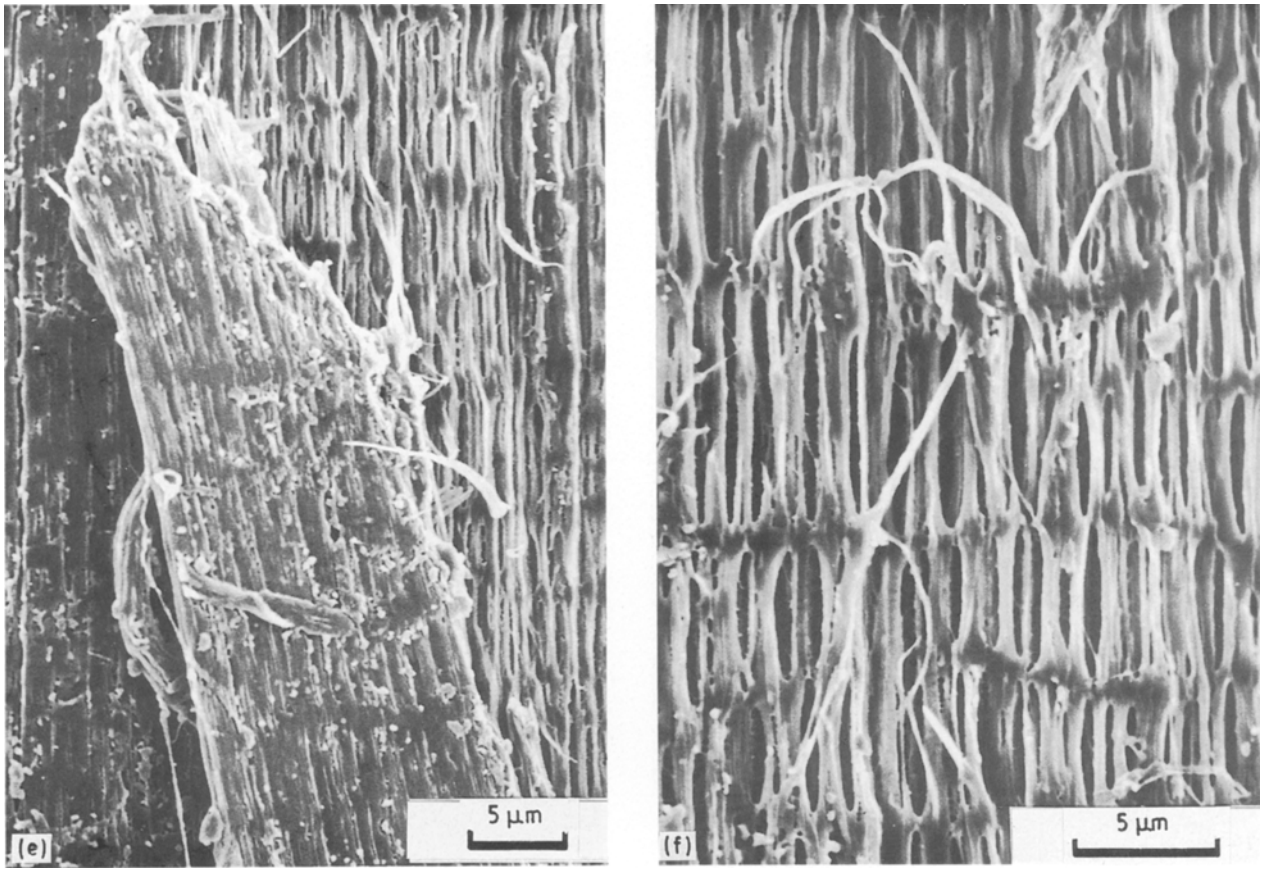

Figure 3. (continued)

sample is too large in diameter to be stretched by a machine. Therefore, attempts were made to observe the fibres immediately freed from tension after stretching. The technique encompasses the problem that the observed void-size is smaller than the true size, owing to stress relaxation of fibrils on removal of the tension. However, if the fracture can be stopped at the level of a minor fracture by load release, information on the initial fracture process can be obtained from change in void shape. This was achieved by stretching the sample at a low crosshead speed.

Fig. 3 shows scanning electron micrographs of the sample thus obtained. No significant changes were found in the surface of the sample stretched under tension below 80% breaking strength (Fig. 3a). This proves the sample to be highly elastic. At 90%, many slender voids parallel to the fibre axis were observed at all points on the surface (Fig. 3b), and fibrillar bands just before fracture which have an inclined shear band at the root were seen in some places (Fig. 3c). At 95% stress, fractured fibrillar bands and their striated traces were observed in several places, in addition to slender voids, but voids or cracks transversally stretched were not observed at all (Fig. 3d). The opposite fractured surface of the fractured fibrillar band in Fig. 3d showed clearly an inclined fracture surface resulting from breaking along the inclined shear band (Fig. 3e). Such an inclined shear band generally appears in necking of polymer materials [32]. The angle of the band in the case of unidirectional stretching, based on the von Mises yield criterion [35], is 54.7°. The angle in the present case was $\sim 50°$, this being within the limits of 50°–57° for the usual polymer fibres [36].

Fig. 3f shows a scanning electron micrograph of the striated trace in Fig. 3d at higher magnification. The necking of fibrils and interfibrillar cavities were observed over the surface. The occurrence of shear bands and necking of fibrils indicates that the surface fracture in the initial stage is mainly due to shear slippage of fibrillar bands. The slender voids and interfibrillar cavities in the stretched samples were apparently formed by stress-rupture of the cross-fibrils separating each microfibril of the unstretched sample. The transformation of the void shape from oval to slender by stretching means that void extension occurs mainly on the fibre axis in the initial stage, or that stress concentration is generated along the fibrillar surface.

3.3. Fractography

Fig. 4 shows scanning electron micrographs of the fractured sample surfaces. The fractured tip split into small fibrils (Fig. 4a) and was curled in appearance, where no voids were observed (Fig. 4b). The splitting of fibrils reached to ~ 50 mm below the top. The curl at the tip was observed over large sectional areas. The shape and size of defects also changed depending on the distance from the top: at a position several tens of micrometres from the top, many microvoids were found between the macrofibrils; at a position several hundreds of micrometres from the top, many slender cavities of ~ 5 μm long and ~ 1 μm wide were seen between the fibrils; below several tens of millimetres

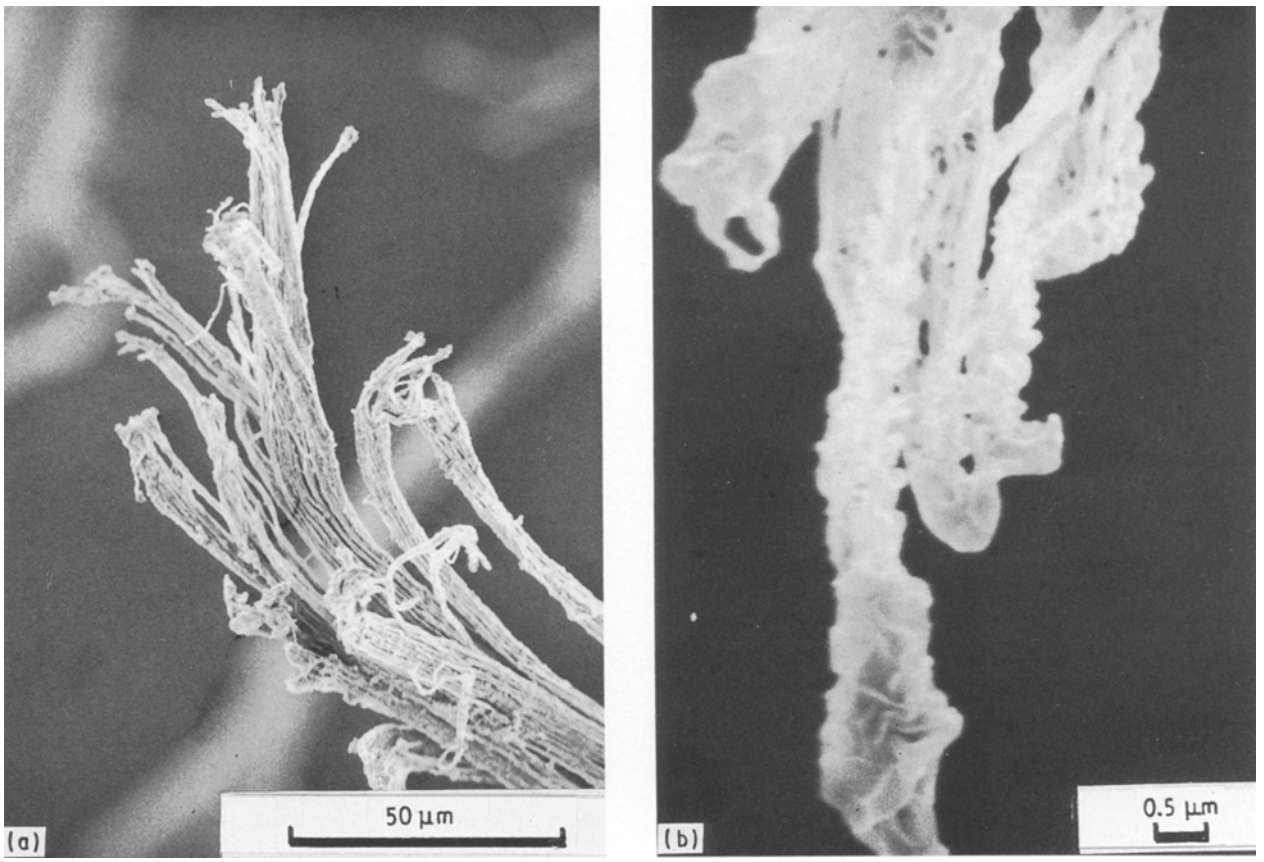

Figure 4 Scanning electron micrographs of the surface of a fractured superdrawn POM fibre: (a) a fractured fibre tip showing a split of fibrils; (b) a fractured fibre tip at higher magnification showing a curl of fibrils and no voids.

from the top, many oval macrovoids were observed in the fibre; and at a greater distance below, buckling slantingly crossing the surface of the sample was seen.

It is supposed that the split at the tip, slender cavities and macrovoids, are due to the applied tensile stress and also a recoil force when the stress is released by a moment of fracture. The buckling arises from the recoil force, because no buckling was observed before fracture. The occurrence of curled fibrils at the tip clearly reveals the fibrils to melt during fracture, i.e. the generation of heat. The curl was observed in almost all sample tips, suggesting that the phenomenon occurs over the cross-section rather than at a local point on the surface. The same phenomenon has been observed for the superdrawn UHMWPE [21, 28], and has been predicted theoretically [24].

The problem of whether the melt is either the main cause or the result of fracture, is important in the study of the fracture phenomenon from basic viewpoints. Necking of fibrils just before fracture may suggest heat generation to result from the elastic strain energy release in the Griffith theory. However, the problem cannot be solved by only the present experiment, because the fracture in the present case includes other possibilities such as phase transition of crystal to melt phase, friction due to shear slippage of fibrils or molecular chains, bond rupture of molecular chains, other processes or combinations of these. The problem remains unresolved at present.

3.4. Fracture process

In the case of superdrawn polyoxymethylene fibrillar fibres, the following fracture process is assumed, on the basis of characteristics of fibrillar structure and deformation behaviour of voids in tension. An applied tensile stress attacks the weakest place in the fibre structure, i.e. a void chain as a structural unit of defects, then dominantly tears cross-fibrils as chains in the void chain, resulting in the generation of macrovoids. The growth of microvoids proceeds in the fibre direction, because thin cross-fibrils, being less resistant to the vertical stress, are dominantly broken rather than the thick fibrils which are much more resistant to the stress; in other words, the microfracture is vertically transmitted through the breakage of the void chain, rather than that of the fibril network in which a much larger stress is required to pierce the thick wall. The network plays the role of stress resistance which prevents lateral development of voids by the thick wall for a short while, as predicted in the theoretical investigation on toughening mechanisms of fibre-reinforced materials [5]. This is the reason why the transformation of microvoids into slender macrovoids was observed before fracture.

The deformation of fibrils is almost elastic under tension below 80% breaking strength but leaves a permanent strain over the tension, i.e. as longitudinal slender voids and cavities at $\sim$ 90%. A greater tension of $\sim$ 95% continuously breaks several fibrillar

networks, i.e. generates a local scission across fibrillar bands. Phenomenologically, the local scission results from fracture of fibrils occurring at necking, where slipping of the fibrils largely contributes to the fracture, because a lack of cross-fibrils connecting the neighbouring fibrils facilitates easy fibrillar slippage. At a greater tension, local breakage in the fibre surface occurs rapidly to the inside, resulting in a catastrophic fracture at maximum stress.

The internal fracture is also supposed to proceed by the same process as on the surface, suggesting a possible dependence of fracture strength on the void size and content. However, the strength of the present fibre was almost independent of these parameters, i.e. levelled off above a draw ratio of 22, as previously reported [37]. This probably arises due to the following two conditions: (1) breakage of voids is transmitted only in the fibre direction until the fracture begins, which is almost independent of the fracture of fibrils parallel to the fibre axis, i.e. strength mainly depends on the thickness of the fibrils; (2) the number of molecular chains which contributes to the strength, i.e. the number of fibrils slipping and/or tie molecular chains per cross-sectional areas, is leveled off in the range of high draw ratios.

The first condition will be attained by the fact that the maximum diameter of voids included in the unstretched drawn fibre is about one-fifth smaller than the thickness of the trunk fibril as the frame holding the fibrillar structure. According to Griffith's theory and weakest link hypothesis, strength is determined by the critical length of the crack and the concentration which can be experimentally obtained. In the present case, the critical diameter of voids was $\sim$ 1.1 μm from the previous result [37], which is comparable to the thickness of the trunk fibril.

This does not ignore the role of branch fibrils in the fracture process. The thickness of branch fibrils is about six times larger than that of cross-fibrils and comparable to void size. Therefore, fracture of branch fibrils follows the breakage of void chains and continues up to the onset of fracture from the frame network. In other words, a sub-network of branch fibrils inside the frame network contributes to homogeneous dispersion of applied stress and prevention of lateral cracking due to cavities. The second condition is not confirmed at present. Levelling the number of tie molecules has been reported with superdrawn POM fibres prepared by a microwave heating/drawing process [38, 39].

However, slippage of fibrils also clearly occurred in the present case. Therefore, the fracture presumably proceeds by a combined process of fibrillar slippage and chain breakage. To obtain greater understanding of the tensile strength, an investigation of the effects of fibrillar size on strength is currently in progress.

4. Conclusions

A fibrillar structure, its deformation under tension and the appearance of the fracture surface of superdrawn polyoxymethylene fibres were examined using scanning electron microscopy. A fracture process was then surmised based on the experimental results, and the following points were elucidated.

1. Fibrillar structure is formed with a complex fibrillar network which consists of fibrils parallel to the fibre axis, cross-fibrils like a ladder between the fibrils and void chains connected to cross-fibrils in the fibre direction. The network is characterized by a frame network of thick fibrils, a sub-network of fibrils branching inside a cell unit which forms the frame, and thin cross-fibrils and voids in the sub-network. Each void is screened with thick fibrils and separated by thin cross-fibrils in directions parallel and perpendicular to the fibre axis, respectively. Also, the fibrillar structure shows a skin/core structure consisting of a dense skin layer at the uppermost surface and a porous core at a more interior point.

2. The fibrillar structure shows different deformation behaviour depending on the number of stretching stages; the deformation of the structure was almost elastic up to 80% breaking strength, produced by an inclined shear band at $\sim$90%, and the breakage of the fibrillar band along the shear band on the surface at $\sim$95%. This arises due to the characteristic fibrillar structure, i.e. the linear void chain (a structural unit of defects) is fragile against tensile stress owing to the thin cross-fibrils being the linking element, but the network of fibrils is very resistant to stress and prevents lateral development of voids by the thick wall. The fracture of void chains is almost independent of the fracture of fibrillar bands, because no lateral cracking resulting from void fracture occurs even in the stage of ultimate fibre fracture.

3. Tensile fracture of superdrawn POM fibres occurs according to the following successive processes: (a) in the initial stage, the void chain breaks dominantly in the fibre direction, resulting in slender macrovoids, leading to cavities between the fibrils. In this stage, the thick fibrils do not fracture, but yield to necking; (b) at a greater tension, the fibrils fracture at the neck, causing a fracture of fibrillar bands on the surface, i.e. a shear-band fracture; (c) the surface fracture develops rapidly to the inside, leading to ultimate fracture. In these processes, a fracture of void chains has little influence on the fibrillar fracture, suggesting the dimension of frame fibrils to be the main factor of tensile strength.

These types of fracture behaviour are well explained by several characteristics of the defect structure, i.e. linear void chains, stress-deformation behaviour in which void fractures are dominantly transmitted in the longitudinal direction but not in the lateral direction, and the extremely small void size compared to the critical diameter of the voids for stress-cracking, which is comparable to the thickness of the frame fibrils. In addition, the slippage of fibrils and the generation of heat clearly occur during this fracture.

References

1. A. A. GRIFFITH, *Phil. Trans. Roy. Soc. London* **221** (1921) 163.
2. E. OROWAN, in "Proceedings of the Symposium on Fatigue and Fracture of Metals" (Wiley, New York, 1950) p. 139.

3. G. R. IRWIN, *J. Appl. Mech.* **24** (1957) 361.
4. J. G. WILLIAMS, *in Advances in Polymer Science* Vol. **27,** (Springer, 1978).
5. F. GUIU and R. N. STEVENS, *J. Mater. Sci.* **26** (1991) 4375.
6. F. T. PEIRCE, *J. Text. Inst.* **17** (1926) 355.
7. W. WEIBULL, *J. Appl. Mech.* **18** (1951) 293.
8. H. D. WAGNER, *J. Polym. Sci. Polym. Phys. Ed.* **27** (1989) 115.
9. A. TOBOLSKY and H. EYRING, *J. Chem. Phys.* **11** (1943) 125.
10. S. N. ZHUKOV and B. N. NARZULLAYEV, *Z. Tech. Phys.* **23** (1953) 1677.
11. F. BUECHE, *J. Appl. Phys.* **26** (1955) 1133.
12. S. N. ZHUKOV, A. Y. SAVOSTIN and E. E. TOMASHEVSKII, *Sov. Phys. Dokl.* **9** (1964) 968.
13. B. A. LLOID, K. L. DEVRIES and M. L. WILLIAMS, *J. Polym. Sci. A2* **10** (1972) 1415.
14. J. H. WENDORFF, *Progr. Colloid Polym. Sci.* **66** (1979) 135.
15. B. D. COLEMAN, *J. Polym. Sci.* **20** (1956) 447.
16. S. N. ZHURKOV and V. E. KORSKOV, *J. Polym. Sci. Phys. Ed.* **12** (1974) 385.
17. J. M. CRISMAN and L. J. ZAPAS, *Polym. Engng Sci.* **19** (1979) 99.
18. Y. TERMONIA, P. MEAKIN and P. SMITH, *Macromolecules* **18** (1985) 2246.
19. T. YOKOBORI, *J. Phys. Sci. Jpn* **10** (1955) 368.
20. D. C. PREVORSEK and J. W. LYONS, *J. Appl. Phys.* **35** (1964) 3152.
21. J. SMOOK, W. HAMERSMA and A. J. PENNINGS, *J. Mater. Sci.* **19** (1984) 1359.
22. A. E. ZACHARIADES and T. KANAMOTO, *J. Appl. Polym. Sci.* **35** (1988) 1265.
23. Y. WADA and A. NAKAYAMA, *ibid.* **15** (1971) 183.
24. K. J. SMITH Jr, *Polym. Engng Sci.* **30** (1990) 437.
25. K. S. MACTURK, R. K. EBY and W. W. ADAMS, *Polymer* **32** (1991) 1782.
26. A. CROSS and R. N. HAWARD, *J. Polym. Sci. Phys. Ed.* **11** (1973) 2423.
27. P. L. CONES, K. SMITH and R. N. HAWARD, *ibid.* **15** (1977) 955.
28. Y. SAKAI and K. MIYASAKA, *Polymer* **31** (1990) 51.
29. W. HOOGSTEEN, H. KORMELINK, G. ESHUIS, G. ten BRINKE and A. J. PENNINGS, *J. Mater. Sci.* **23** (1988) 3467.
30. M. HOFF and Z. PELZBAUER, *Polymer* **32** (1991) 999.
31. D. C. PREVORSEK, P. J. HARGET, R. K. SHAMA and A. C. REIMSCHUESSEL, *J. Macromol. Sci. Phys.* **B8** (1973) 127.
32. P. SMITH, P. J. LEMSTRA, J. P. L. PIJPERS and A. M. KIEL, *Coll. Polym. Sci.* **259** (1981) 1070.
33. R. J. MORGAN, C. D. PRUNEDA and W. J. STEELE, *J. Polym. Sci. Phys. Ed.* **21** (1983) 1757.
34. T. KOMATSU, S. ENOKI and A. AOSHIMA, *Polymer* **32** (1991) 1983.
35. R. von MISES, *Nachr. Ges. Wiss. Gott.* **1** (1913) 582.
36. M. ISIKAWA, I. NARISAWA and H. OGAWA, *Polym. J.* **8** (1976) 391.
37. T. KOMATSU, S. ENOKI and A. AOSHIMA, *Polym.*, **33** (1992) 2123.
38. Y. TAKEUCHI, F. YAMAMOTO and K. NAKAGAWA, *J. Polym. Sci. Polym. Phys. Ed.* **23** (1985) 1193.
39. W. P. LEUNG and C. L. CHOY, *ibid.* **25** (1987) 2059.

Received 10 April
and accepted 29 October 1992